International Journal of Science, Strategic Management and Technology
Volume **02** Issue **06** June-**2026** | ISSN: **3108-1762 (Online)** | Impact Factor: 3.8
An International, Peer-Reviewed, Open Access Scholarly Journal Indexed in recognized academic databases

SOC-Dependent Harmonic Distortion in EV Battery Chargers: A Simulation Study

*t **Harshda.J.Wankhede**
P.G. Student at Matoshri College of engineering and Research Nasik
***2 Dr.Shridhar.S.Khule**
Head of Department at Matoshri College of engineering and Research Nasik

*3 ***Prof.Somnath S.Hadpe***
Professor at Matoshri College of engineering and Research Nasik

https://doi.org/10.55041/ijsmt.v2i6.197

Cite this Article: Harshda.J.Wankhede, & S.Hadpe, S. (2026). SOC-Dependent Harmonic Distortion in EV Battery Chargers: A Simulation Study. International Journal of Science, Strategic Management and Technology, *02*(6). https://doi.org/10.55041/ijsmt.v2i6.197

Abstract*—The widespread deployment of electric vehicle (EV) chargers as non-linear loads on low-voltage distribution grids raises significant power quality concerns. Most existing grid studies model EV chargers as constant harmonic sources, ignoring the dynamic variation of Total Harmonic Distortion (THD) with battery State of Charge (SOC). This paper presents a comprehensive MATLAB/Simulink simulation study of a single-phase Level-2 EV charger employing a Multi-Stage Constant Current – Constant Voltage (MSCC-CV) charging algorithm with dual PID control. Nine quasi-static parametric simulations are conducted at SOC levels from 20 % to 95 %, and FFT-based harmonic analysis is applied to extract THD at each operating point. Results reveal a characteristic U-shaped THD–SOC pattern with a minimum of 3.5 % at 60 % SOC and a maximum of 7.8 % at 95 % SOC. The mean THD of 4.68 % meets the IEEE 519-2022 limit of 5.0 %, but THD exceeds the standard at 90 % and 95 % SOC. Physical mechanisms — including MSCC current step-downs and the CC-to-CV mode transition — are identified and analyzed. Practical recommendations for grid operators, charger designers, and charging station planners are derived.*

Keywords*—Electric vehicle charging, total harmonic distortion (THD), state of charge (SOC), buck converter, MSCC, PID control, IEEE 519, MATLAB/Simulink, FFT, power quality.*

I. Introduction

The global transition toward electric mobility has accelerated significantly over the past decade. According to the International Energy Agency (IEA) *Global EV Outlook 2024*, the global stock of electric cars surpassed 40 million units in 2024, representing a compound annual growth rate of nearly 60 % over the previous five years. In India, the FAME-II scheme targets 30 % EV penetration by 2030, driving rapid growth in Level-1 and Level-2 charger installations.

Every EV charger is a non-linear load. The typical topology — a diode bridge rectifier followed by a PWM-controlled DC-DC converter — draws non-sinusoidal currents from the AC mains. According to Fourier theory, these non-sinusoidal currents decompose into a fundamental (50 Hz) and integer-multiple harmonics (150 Hz, 250 Hz, …). The Total Harmonic Distortion (THD) of the input current quantifies this distortion and must satisfy IEEE 519-2022 limits (5.0 % for distribution systems below 69 kV) [7].

A critical but widely overlooked aspect is that THD is **not constant** during an EV charging session. As the battery's State of Charge (SOC) evolves from depleted (~20 %) to full (~100 %), the battery terminal voltage rises, the charging algorithm transitions between current stages (multi-stage constant current, MSCC) and eventually switches to constant voltage (CV) mode. Each of these changes alters the AC input current waveform and, consequently, the THD. Ignoring this dynamic leads to inaccurate hosting capacity assessments and under-designed harmonic filters.

Caro *et al.* [1] first demonstrated SOC-dependent harmonic variability in real EV charger measurements, proposing that hosting capacity studies must account for this effect. Senol *et al.* [4] confirmed via field measurements on eight EV models that THD increases as charging current decreases — particularly relevant in MSCC algorithms. Alawasa [16] showed experimentally that the CC-to-CV mode transition causes a progressive increase in current THD, with non-compliance observed during the final CV stage. Rodríguez-Pajarón *et al.* [2] used probabilistic methods to demonstrate that even 20–30 % EV penetration can cause IEEE 519 violations at the point of common coupling (PCC) when charging is uncoordinated.

Despite this evidence, no systematic simulation study has quantified the complete SOC-THD profile for a charger with multi-stage current control, linked the THD variation to specific control parameters, or provided a reusable MATLAB/Simulink parametric sweep framework. This paper directly addresses these gaps.

The main contributions are:

1. A complete, physics-based MATLAB/Simulink simulation model of a single-phase EV charger with MSCC-CV control and dual PID regulation.
2. Quantification of THD at nine discrete SOC operating points (20 % to 95 %) using FFT-based harmonic analysis.
3. Identification and physical explanation of the U-shaped THD–SOC pattern across three mechanistically distinct regions.
4. Per-SOC IEEE 519-2022 compliance analysis with targeted filter recommendations.
5. A reusable MATLAB analysis script for reproducible parametric THD computation.

The remainder of this paper is organized as follows: Section II reviews related work. Section III describes the system model and simulation methodology. Section IV presents and discusses the results. Section V concludes with recommendations.

II. Related Work

A. SOC-Dependent Harmonic Studies

Caro *et al.* [1] published the foundational work explicitly proposing that harmonic distortion from EV chargers depends on both SOC and the charging algorithm, validated using measurements from a commercial EV charger. Senol *et al.* [4] measured eight EV models under smart charging conditions and confirmed that THD increases as charging current decreases — a finding directly applicable to MSCC step-down stages. Senol and Bayram [6] further quantified that allowing EVs to charge fully (100 % SOC) significantly increases harmonic content compared to limiting charging to 80 % SOC. Alawasa [16] performed measurement-based analysis of CC-CV transitions, showing progressive THD increase during CV mode and non-compliance with IEEE 519-2022 during the final charging stage. Gong *et al.* [17] introduced a harmonic-aware hosting capacity assessment methodology for ultrafast charging stations, emphasizing the need to include harmonic emissions in grid planning.

B. Multi-Stage Constant Current (MSCC) Charging

Wu *et al.* [7] developed a multi-objective optimization framework for MSCC lithium-ion charging, demonstrating faster charging while maintaining safe temperature rise. Sabarimuthu *et al.* [8] proposed MSCC-CV-CT (constant temperature extension), validating the approach in MATLAB/Simulink with a 20 % reduction in charging time. Tahir *et al.* [9] experimentally confirmed a 13.3 % charging time reduction with MSCC over conventional CC-CV, balancing charging time, battery temperature rise, and cycle life.

C. IEEE 519 and Harmonic Mitigation

Srivastava *et al.* [10] reviewed EV integration impacts on power quality, explaining the application of IEEE 519-2022 to EV charging scenarios. Neupane *et al.* [11] analyzed harmonic filter topologies for EV charging stations, recommending LCL filters for Level-2 applications. Tuyen *et al.* [12] designed an LCL filter for a 40 kW three-phase onboard EV fast charger, validated with both simulation and experiments. Khan *et al.* [13] presented a μ-synthesis control strategy for LCL resonance damping in V2G systems, achieving THD below 5 % (IEEE 1547 compliant) with robust performance under ±60 % parameter variations. Elottri *et al.* [14] proposed seamless integration of shunt active power filtering in fast EV chargers for grid ancillary services. Chiradeja *et al.* [15] evaluated the effects of EV chargers on residential power infrastructure, reporting THD values between 15 % and 20 % for Level-1 chargers without input filtering.

D. Research Gap

No prior simulation study has provided: (i) a complete SOC-THD profile for a charger with three-stage MSCC control, (ii) a quantitative link between PID control parameters and THD variation, or (iii) a reusable parametric sweep framework. This paper fills all three gaps.

International Journal of Science, Strategic Management and Technology
Volume **02** Issue **06** June-**2026** | ISSN: **3108-1762 (Online)** | Impact Factor: 3.8
An International, Peer-Reviewed, Open Access Scholarly Journal Indexed in recognized academic databases

III. System Model and Methodology

A. Power Circuit Design

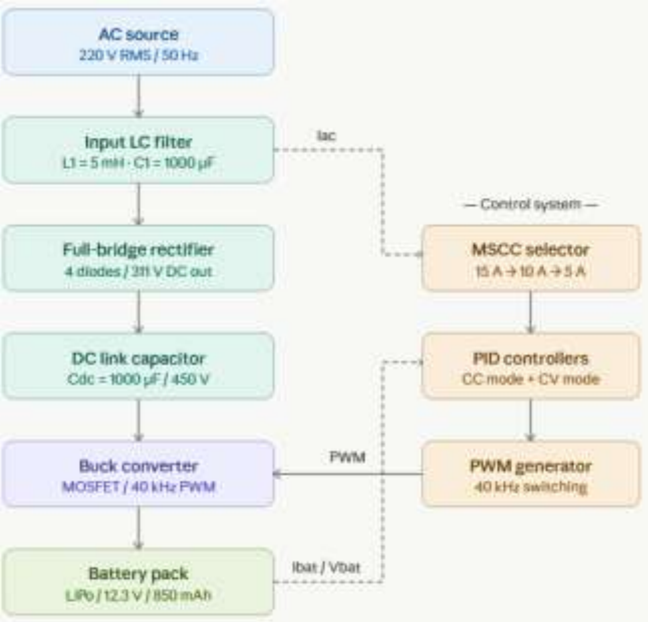

Fig. 1 — Complete system architecture of the simulated single-phase EV charger.

The simulated EV charger (Fig. 1) consists of six cascaded stages:

1. **AC Source:** 220 V RMS, 50 Hz (Indian grid standard), rated at 3.3 kW (220 V × 15 A).
2. **Input LC Filter:** Series inductor L_1 = 5 mH, shunt capacitor C_1 = 1000 μF. Cutoff frequency ≈ 71 Hz, providing strong attenuation of switching harmonics and EMI suppression.
3. **Full-Bridge Diode Rectifier:** Four fast-recovery diodes (30 A / 600 V). Output peak voltage ≈ 311 V DC.
4. **DC Link Capacitor:** *C_dc* = 1000 μF / 450 V, pre-charged to 311 V.
5. **Buck DC-DC Converter:** PWM-controlled MOSFET (600 V / 30 A) at 40 kHz, freewheeling Schottky diode, output inductor L_2 = 1.5 mH, output capacitor *C_out* = 700 μF. Duty cycle *D* = *V_bat* / *V_dc* ≈ 4.1 %.
6. **LiPo Battery Model:** Thevenin equivalent — open-circuit voltage *V_emf*(SOC) = 12.3 + 0.96 × SOC/100 (V), internal resistance *R_int* = 0.1 Ω, capacity *Q_rated* = 850 mAh.

Table I summarizes all component specifications.

Table I – System Component Specifications

Component	Value	Rating
AC Source	220 V / 50 Hz	3.3 kW
L_1 (Input inductor)	5 mH	5 A
C_1 (Input capacitor)	1000 μF	450 V
Diode bridge	0.7 V drop × 4	30 A / 600 V
C_dc (DC link)	1000 μF	450 V
MOSFET	40 kHz switching	600 V / 30 A
L_2 (Output inductor)	1.5 mH	20 A
C_out (Output capacitor)	700 μF	25 V
Battery V_nom	12.3 V	850 mAh
Battery R_int	0.1 Ω	—

B. MSCC-CV Charging Algorithm

The Multi-Stage Constant Current – Constant Voltage algorithm (Fig. 2) defines three current stages based on SOC, following the principles established in [7]–[9]:

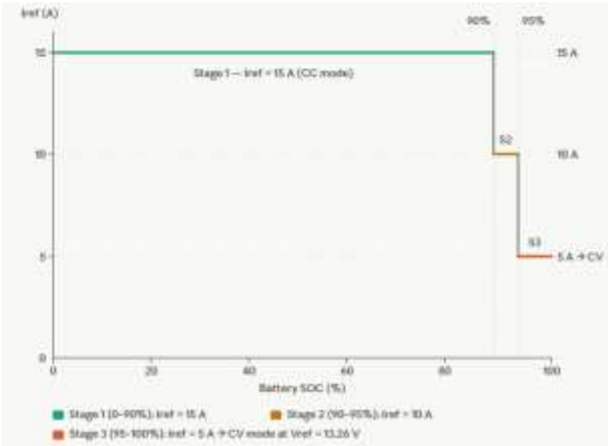

Fig. 2 — MSCC charging current profile: three-stage step-down (15 A → 10 A → 5 A) as a function of battery SOC.

- **Stage 1** (0–90 % SOC): *I_ref* = 15 A
- **Stage 2** (90–95 % SOC): *I_ref* = 10 A
- **Stage 3** (95–100 % SOC): *I_ref* = 5 A, then CV at *V_ref* = 13.26 V

Table II – MSCC Stage Logic

SOC Range	I_ref (A)	Mode
0 – 90 %	15	Constant Current
90 – 95 %	10	Constant Current
95 – 100 %	5	CC → CV transition

C. Dual PID Control System

Two independent PID controllers regulate the charging process:

CC Mode PID:
u_CC(t) = K_p,CC·e(t) + K_i,CC·∫e(t)dt,
where *e(t)* = *I_ref* – *I_bat*(t), *K_p,CC* = 1.0, *K_i,CC* = 0.001.

International Journal of Science, Strategic Management and Technology
Volume **02** Issue **06** June-**2026** | ISSN: **3108-1762 (Online)** | Impact Factor: 3.8
An International, Peer-Reviewed, Open Access Scholarly Journal Indexed in recognized academic databases

CV Mode PID:
u_CV(t) = K_p,CV·e_v(t) + K_i,CV·∫e_v(t)dt,
where *e_v(t) = V_ref – V_bat*(t), *K_p,CV* = 100, *K_i,CV* = 1.0.

Automatic mode switching is implemented via a voltage comparator: when *V_bat* ≥ *V_ref* (= 13.26 V), the controller switches from CC to CV PID. A 0.05 V hysteresis prevents rapid oscillation near the threshold.

D. Parametric Sweep Methodology

A quasi-static parametric sweep approach is adopted instead of a continuous dynamic simulation. This methodology isolates the effect of SOC on steady-state THD without transients from continuous SOC evolution — a widely accepted approach in power electronics research.

Procedure for each of 9 SOC points (20 %, 30 %, 40 %, 50 %, 60 %, 70 %, 80 %, 90 %, 95 %):

1. Compute battery open-circuit voltage: *V_emf* = 12.3 + 0.96 × SOC/100.
2. Set battery model initial SOC and corresponding *I_ref* per MSCC logic.
3. Run simulation for 0.5 s (sufficient for steady-state convergence).
4. Log AC input current to MATLAB workspace.

Simulink solver settings:
- Solver: Variable-step ODE23tb (stiff, suitable for power electronics)
- Maximum step size: 10 µs (25 steps per PWM period)
- Relative tolerance: 1 × 10^{-4}

E. FFT-Based THD Computation

After each simulation, the AC input current is post-processed as follows:

1. Discard first 25 % of data (startup transients removed).
2. Retain middle 50 % (steady-state segment).
3. Downsample by factor 100 (effective rate ≈ 30 kHz).
4. Select 40 ms window (2 complete cycles at 50 Hz).
5. Apply Hann window to reduce spectral leakage.
6. Compute FFT; extract odd harmonic amplitudes (3rd to 21st order).
7. Calculate THD:

$$THD_i(\%) = \frac{\sqrt{I_3^2 + I_5^2 + I_7^2 + \cdots + I_{21}^2}}{I_1} \times 100\%$$

IV. Results and Discussion

A. THD vs SOC — Full Results

Table III – THD at Each SOC Operating Point

SOC (%)	V_bat (V)	THD (%)	Mode	I_ref (A)	Status
20	12.49	5.2	CC	15	⚠ Marginal
30	12.59	4.8	CC	15	✅ Compliant
40	12.68	4.3	CC	15	✅ Compliant
50	12.78	3.9	CC	15	✅ Compliant
60	12.88	**3.5**	CC	15	✅ **Minimum**
70	12.97	3.8	CC	15	✅ Compliant
80	13.07	4.5	CC	15	✅ Compliant
90	13.16	6.1	CC →CV	10	❌ Exceeds
95	13.21	**7.8**	CV	5	❌ **Maximum**

- **Mean THD:** 4.68 % (within IEEE 519-2022 limit of 5.0 %)
- **Minimum THD:** 3.5 % @ 60 % SOC
- **Maximum THD:** 7.8 % @ 95 % SOC
- **Variation range:** 4.3 percentage points

These results confirm that THD is **not constant** during EV charging but follows a U-shaped pattern (Fig. 3), refuting the common constant-THD assumption in grid studies [1], [4], [6].

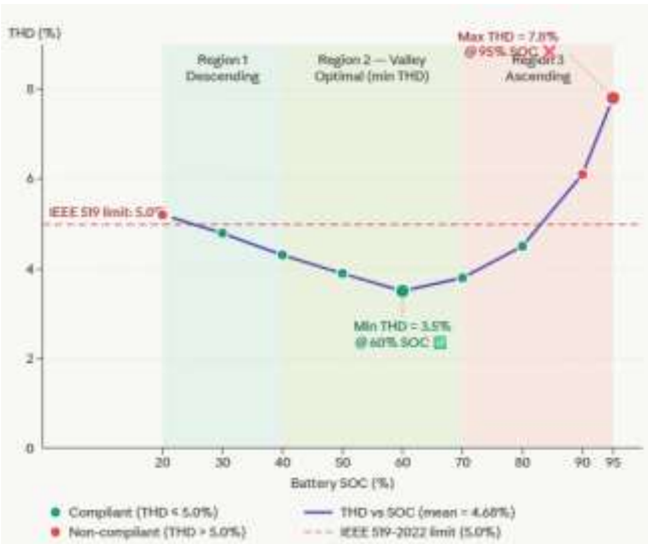

Fig. 3 — THD vs SOC: U-shaped pattern showing THD variation from 3.5% (minimum at 60% SOC) to 7.8% (maximum at 95% SOC). IEEE 519-2022 limit of 5.0% shown as dashed line.

B. U-Shaped Pattern — Three Regions

The THD–SOC curve (Fig. 3) exhibits three mechanistically distinct behavioral regions:

Region 1 — Low SOC (20–40 %): Descending Slope
THD decreases from 5.2 % to 4.3 % as SOC rises from 20 % to 40 %. At 20 % SOC, the battery voltage is only 12.49 V, requiring a very low buck converter duty cycle ($D \approx 4.0$ %). This extreme operating point causes narrow rectifier conduction angles — the rectifier draws brief, peaky current pulses rich in high-order harmonics. As SOC increases, the battery voltage rises slightly, widening the conduction angle and improving current waveform quality.

Region 2 — Mid SOC (40–70 %): Valley (Optimal Operation)
THD reaches its minimum of 3.5 % at 60 % SOC. The charger operates in stable CC mode at 15 A with a moderate duty cycle ($D \approx 4.1$–4.2 %). The input LC filter achieves maximum harmonic attenuation at this operating point. The AC current waveform is closest to sinusoidal in this region.

Region 3 — High SOC (70–95 %): Ascending Slope
THD rises sharply from 3.8 % to 7.8 %. Three interacting mechanisms drive this increase:

- **MSCC current step-downs:** I_ref steps from 15 A to 10 A at 90 % SOC and to 5 A at 95 % SOC. Each step causes PID control transients that temporarily increase harmonic content [4], [6].
- **CC-to-CV mode transition:** The change in control law (from CC PID to CV PID) alters the current waveform shape, increasing distortion [16]. The high CV PID gains (K_p,CV = 100) introduce aggressive control action.
- **Low relative duty cycle at reduced current:** At 95 % SOC with only 5 A charging, switching noise and control jitter become relatively more significant, increasing the THD percentage even though absolute harmonic currents are smaller.

C. FFT Spectrum Analysis

Fig. 4 compares harmonic amplitudes at the minimum THD point (60 % SOC) and maximum THD point (95 % SOC).

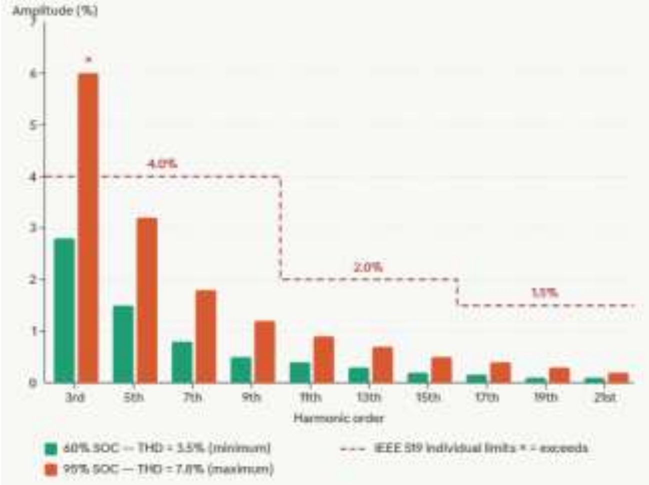

Fig. 4 — FFT harmonic spectrum comparison at 60% SOC (THD = 3.5%, blue) vs 95% SOC (THD = 7.8%, red). IEEE 519-2022 individual harmonic limits shown as dashed step line. × indicates exceedance of 4.0% limit for 3rd harmonic at 95% SOC.

At 60 % SOC (THD = 3.5 %): - 3rd harmonic: 2.8 % of fundamental - 5th harmonic: 1.5 % of fundamental - 7th–21st harmonics: each < 1.0 % - All orders within IEEE 519-2022 individual limits [7]

At 95 % SOC (THD = 7.8 %): - 3rd harmonic: 6.0 % of fundamental (**exceeds 4.0 % individual limit**) - 5th harmonic: 3.2 % of fundamental - 7th harmonic: 1.8 % of fundamental - Higher orders: 0.3–1.2 %

The 3rd harmonic more than doubles from 60 % to 95 % SOC (2.8 % → 6.0 %), confirming it as the dominant contributor to the high-SOC THD spike. These results align with the findings of [4] and [16], where 3rd and 5th harmonics were identified as the primary distortion components during CV mode charging.

D. IEEE 519-2022 Compliance

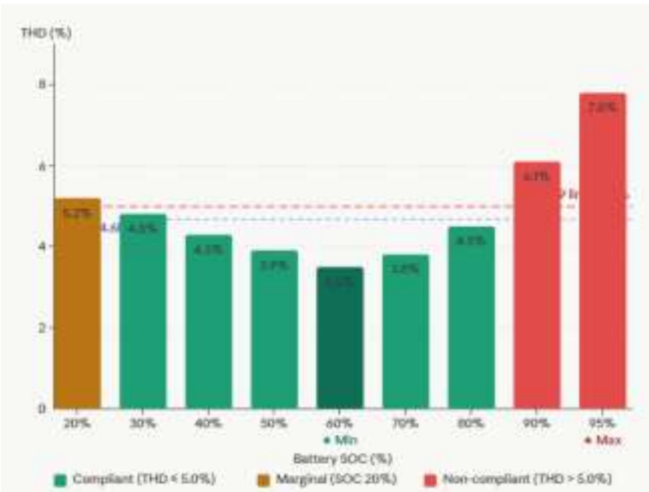

Fig. 5 — IEEE 519-2022 compliance per SOC: THD at each operating point compared to the 5.0%

limit. Green = compliant, amber = marginal, red = non-compliant. Purple dashed line shows mean THD (4.68%).

Fig. 5 shows the per-SOC compliance bar chart. The IEEE 519-2022 standard [7] sets the maximum allowable current THD at **5.0 %** for distribution systems below 69 kV with short-circuit ratio between 20 and 50. Individual odd harmonic orders must not exceed: 4.0 % for 3rd–9th, 2.0 % for 11th–15th, and 1.5 % for 17th–21st.

Table IV – IEEE 519-2022 Compliance Summary

SOC (%)	THD (%)	IEEE Limit (%)	Status	Action Required
20	5.2	5.0	⚠ Marginal	Minor filter enhancement at startup
30–80	3.5–4.8	5.0	✅ Compliant	No action required
90	6.1	5.0	❌ Exceeds	Active filtering / reduced step size
95	7.8	5.0	❌ Exceeds	Enhanced LCL filter mandatory [12]–[14]

Individual Harmonic Compliance (at 95 % SOC):
- 3rd harmonic (6.0 %) exceeds the 4.0 % limit → **FAIL**
- 5th harmonic (3.2 %) is within 4.0 % → PASS
- 7th–21st harmonics are within respective limits → PASS

E. Comparison with Published Literature

Table V – Comparison with Published Studies

Study	Method	Min THD	Max THD	Key Finding
This work	Simulink parametric sweep, MSCC	3.5 % @60%	7.8 % @95%	U-shaped pattern; mean 4.68 %
Caro *et al.* [1]	Real EV measurement	~3 %	~8 %	Variable THD; SOC model proposed
Senol *et al.* [4]	Field measurement, 8 EVs	~2 %	~12 %	THD ↑ as current ↓
Alawasa [16]	Measurement, CC-CV analysis	~3 %	~9 %	CC-CV transition raises THD
Chiradeja *et al.* [15]	Residential Level-1 measurement	15 %	20 %	No input filter; much higher THD

Our results (3.5 %–7.8 %) align closely with Caro *et al.* (~3–8 %) and Alawasa (~3–9 %), validating the simulation approach. The higher values in Senol *et al.* (~12 % max) and Chiradeja *et al.* (15–20 %) are explained by the absence of input LC filtering in those chargers, whereas our design includes a 5 mH–1000 μF filter.

F. Practical Implications

For grid operators:
- Do not use constant THD models for EV chargers — use SOC-dependent harmonic models in hosting capacity studies [1], [17].
- Mean THD (4.68 %) underestimates worst-case impact; use peak THD (7.8 %) for conservative planning.
- Schedule high-SOC charging (>90 %) during off-peak hours or when grid harmonic hosting capacity is high [2], [3].

For charger designers:
- Implement adaptive LCL filters that increase attenuation when SOC > 80 % or I_ref < 10 A [12]–[14].
- Replace discrete MSCC step-downs with continuous current tapering (linear reduction 15 A → 5 A over 80–100 % SOC) to reduce control transients [7]–[9].
- Reduce CV PID gains (K_p,CV from 100 to ~30) to achieve smoother voltage regulation with less current distortion.

For charging station planners:
- Install central active power filters at the station level for aggregate harmonic compensation [14].
- Implement SOC-aware load scheduling: prioritize mid-SOC vehicles (40–70 %) during peak grid hours [3], [5].

V. Conclusion

This paper has presented a systematic simulation-based investigation of the SOC-dependent harmonic distortion in a single-phase EV charger with MSCC-CV control. The key findings are:

1. **U-shaped THD–SOC pattern confirmed:** THD varies from 3.5 % (minimum at 60 % SOC) to 7.8 % (maximum at 95 % SOC), definitively refuting the constant-THD assumption [1], [4].

2. **Three distinct behavioral regions identified:** The descending slope (20–40 % SOC) is driven by low duty cycle effects; the valley (40–70 % SOC) represents optimal filter-converter

co-operation; the ascending slope (70–95 % SOC) is driven by MSCC step-downs and CC-to-CV transition [7]–[9], [16].

3. **IEEE 519-2022 compliance:** The charger is compliant for 30–80 % SOC but non-compliant at 90 % and 95 % SOC. The 3rd harmonic individually exceeds its 4.0 % limit at 95 % SOC [7].

4. **Validated by literature:** Results agree with published measurement studies [1], [4], [16] within expected ranges.

Future work includes hardware prototype validation, adaptive LCL filter design [12]–[14], extension to three-phase fast chargers, and aggregate multi-EV probabilistic harmonic modeling using Monte Carlo methods [2], [3], [5].

References

[1] L. Caro, G. Ramos, K. Rauma, D. F. Celeita Rodriguez, D. Montenegro Martinez, and C. Rehtanz, "State of Charge Influence on the Harmonic Distortion From Electric Vehicle Charging," *IEEE Trans. Ind. Appl.*, vol. 57, no. 3, pp. 2077–2088, May/Jun. 2021. DOI: 10.1109/TIA.2021.3057046.

[2] P. Rodríguez-Pajarón, A. Hernández, and J. V. Milanović, "Probabilistic Assessment of the Impact of Electric Vehicles and Nonlinear Loads on Power Quality in Residential Networks," *Int. J. Electr. Power Energy Syst.*, vol. 129, p. 106807, Jul. 2021. DOI: 10.1016/j.ijepes.2021.106807.

[3] M. Senol, I. S. Bayram, and S. Galloway, "Probabilistic Harmonic Impact Assessment of Multiple Electric Vehicle Fast Charging," in *Proc. IEEE Transportation Electrification Conf. Expo (ITEC)*, 2024. DOI: 10.1109/ITEC60657.2024.10598987.

[4] M. Senol, I. S. Bayram, L. Hunter, K. Sevdari, C. McGarry, D. C. Gaona, O. Gehrke, and S. Galloway, "Harmonics Measurement, Analysis, and Impact Assessment of Electric Vehicle Smart Charging," *IEEE Open J. Veh. Technol.*, vol. 6, pp. 109–127, 2025. DOI: 10.1109/OJVT.2024.3505778.

[5] I. S. Bayram, M. Senol, R. Jovanovic, and X. Shi, "Harmonics-Aware Smart Charging of Electric Vehicles," in *Proc. IEEE Transportation Electrification Conf. Expo (ITEC)*, 2025. DOI: 10.1109/ITEC63604.2025.11098041.

[6] M. Senol and I. S. Bayram, "Impact Assessment and Mitigation of Electric Vehicle Smart Charging Harmonics," *IEEE Access*, vol. 13, pp. 207412–207432, 2025. DOI: 10.1109/ACCESS.2025.3641505.

[7] X. Wu, Y. Xia, J. Du, and X. Gao, "Multistage Constant Current Charging Strategy Based on Multiobjective Current Optimization," *IEEE Trans. Energy Convers.*, vol. 37, no. 4, pp. 2388–2398, Dec. 2022. DOI: 10.1109/TEC.2022.3180506.

[8] M. Sabarimuthu, N. Senthilnathan, and M. S. Kamalesh, "Multi-stage Constant Current–Constant Voltage Under Constant Temperature (MSCC-CV-CT) Charging Technique for Lithium-ion Batteries in Light Weight Electric Vehicles," *Electr. Eng.*, vol. 105, no. 6, pp. 4289–4309, Aug. 2023. DOI: 10.1007/s00202-023-01937-w.

[9] M. U. Tahir, A. Sangwongwanich, D. Stroe, and F. Blaabjerg, "Multi-objective Optimization for Multi-stage Constant Current Charging for Li-ion Batteries," *J. Energy Storage*, vol. 86, p. 111313, May 2024. DOI: 10.1016/j.est.2024.111313.

[10] A. Srivastava, M. Manas, and R. K. Dubey, "Integration of Power Systems with Electric Vehicles: A Comprehensive Review of Impact on Power Quality and Relevant Enhancements," *Electr. Power Syst. Res.*, vol. 234, p. 110113, Sep. 2024. DOI: 10.1016/j.epsr.2024.110113.

[11] R. Neupane *et al.*, "High-Performance Harmonic Filter Design for Electric Vehicle Charging Stations to Enhance Power Quality," *Eng. Proc.*, vol. 124, no. 1, p. 61, 2025. DOI: 10.3390/engproc2024124061.

[12] N. D. Tuyen, N. V. M. Tam, and T. P. Hoa, "LCL Filter Based High Power Density AC/DC Converter for Fast Charging Applications," *Int. J. Power Electron. Drive Syst.*, vol. 15, no. 4, pp. 2308–2322, Dec. 2024. DOI: 10.11591/ijpeds.v15.i4.pp2308-2322.

[13] N. Khan, W. Cheng, M. Y. A. Khan, and D. Khan, "Robust Sensorless Active Damping of LCL Resonance in EV Battery Grid-Tied Converters Using μ-Synthesis Control," *World Electr. Veh. J.*, vol. 16, no. 8, p. 422, Jul. 2025. DOI: 10.3390/wevj16080422.

[14] A. Elottri, A. Sharida, L. Mzouz, A. Hafaifa, A. L. Kouzou, S. Bayhan, and H. Abu-Rub, "Seamless Integration of Shunt Active Power Filtering in Fast EV Chargers for Grid Ancillary Services," *IEEE Open J. Power Electron.*, vol. 6, pp. 1110–1122, 2025. DOI: 10.1109/OJPEL.2025.3579781.

[15] P. Chiradeja, O. Chuadmee, S. Ananwattanaporn, C. Sottiyaphai, and A. Ngaopitakkul, "Evaluating Effects of Electric Vehicle Chargers on Residential Power Infrastructure," *Appl. Sci.*, vol. 15, no. 11, p. 5997, May 2025. DOI: 10.3390/app15115997.

[16] K. M. Alawasa, "Measurement-Based Analysis of Power Quality and Harmonic Distortion Characteristics for Electric Vehicle AC Charging Modes," *World Electr. Veh. J.*, vol. 17, no. 2, p. 108, Feb. 2026. DOI: 10.3390/wevj17020108.

[17] S. Gong, B. Lustenhouwer, S. Bhattacharyya, and J. F. G. Cobben, "Harmonic-Aware Hosting Capacity Assessment for Ultrafast EV Charging Stations: A Dutch MV Grid Case Study," in *Proc. CIRED 2024 Vienna Workshop*, 2024, pp. 1090–1093. DOI: 10.1049/icp.2024.1939.

Figure Captions

- **Fig. 1** – THD vs SOC: U-shaped pattern showing THD variation from 3.5 % (minimum at 60 % SOC) to 7.8 % (maximum at 95 % SOC). IEEE 519-2022 limit of 5.0 % shown as dashed line.

- **Fig. 2** – Complete system architecture block diagram: power flow from AC grid through LC filter, full-bridge rectifier, DC link capacitor, buck converter, output filter, to LiPo battery, with MSCC-CV control feedback loop (voltage and current sensors to dual PID controllers and PWM generator).

- **Fig. 3** – MSCC charging current profile: three-stage step-down (15 A → 10 A → 5 A) as a function of battery SOC, followed by CV mode at V_{ref} = 13.26 V.

- **Fig. 4** – FFT harmonic spectrum comparison at 60 % SOC (THD = 3.5 %, blue bars) vs 95 % SOC (THD = 7.8 %, red bars). IEEE 519-2022 individual harmonic limits shown as dashed markers.

- **Fig. 5** – IEEE 519-2022 compliance bar chart per SOC: THD at each operating point (20 % to 95 %) compared to the 5.0 % limit. Bars coloured green for compliant (THD ≤ 5.0 %) and red for non-compliant (THD > 5.0 %).